International Journal of Recent Engineering Research and Development (IJRERD)
Volume No. 02 – Issue No. 01, ISSN: 2455-8761
www.ijrerd.com, PP. 94-105

IR spectral properties and vibrational modes of $[(1x)\{0.75Tl_2HgI_4:0.25AgI\}:xHgI_2]$ nano composite fast ion conductor (where x = 0.2, 0.4, 0.6 and 0.8 mol. wt. %)

Noorussaba[a]*, Afaq Ahmad[a]
[a]*Solid State Chemistry Lab, Department of Chemistry,*
Aligarh Muslim University, Aligarh- 202002, India

Abstract: The novel composite fast ion conducting system $[(1-x)\{0.75Tl_2HgI_4:0.25AgI\}:xHgI_2]$ (where x = 0.2, 0.4, 0.6 and 0.8 mol. wt. %) were prepared and characterized by IR spectroscopy. The IR spectra of $[(1-x)\{0.75Tl_2HgI_4:0.25AgI\}:xHgI_2]$ (where x = 0.2, 0.4, 0.6 and 0.8 mol. wt. %) have been measured in different scattering orientations covering the successive phase transitions down to 473K. $[(1-x)\{0.75Tl_2HgI_4:0.25AgI\}:xHgI_2]$ (where x = 0.2, 0.4, 0.6 and 0.8 mol. wt. %). This work suggests that thallium (I) ionic conductors may exist, analogous to some well-known double salt conductors based on simple silver (I) and copper (I) halides. In addition, the present study demonstrates the usefulness of IR spectroscopy in the characterization of heavy metal ionic conductors. The mobility of Tl^+ in halide compounds has been investigated to develop an understanding of the factors which are important in fast ion conduction. These compounds are characterized by transitions at elevated temperatures to disordered phases in which the M^+ ion is highly mobile. Trends in the transition temperatures, conductivities, and activation energies for ion transport demonstrate that Tl^+ are less mobile than Cu and Ag^+. The crystal structure of the low-temperature phase of $[(1-x)\{0.75Tl_2HgI_4:0.25AgI\}:xHgI_2]$ (where x = 0.2, 0.4, 0.6 and 0.8 mol. wt. %) has been determined at 200°C. The Hg^+ ions are tetrahedrally coordinated by I^- ions. The TI^+ ions are found to reside in seven-coordinate sites approximating C_{2v}, capped trigonal prisms. There is no clear-cut migration path for the Tl^+ ions, but some plausible conduction mechanisms are discussed.

Keywords: Synthesis, Fourier transmission infrared spectra (FTIR), phase transition, Doping, Fast ion conductor.

1. Introduction

During the past few years there has been increasing interest in a class of ionic solids which exhibit high ionic conductivity far below their melting points. These solids have come to be called solid electrolytes or superionic conductors. They have a rigid sublattice of one species creating many vacant sites for highly mobile ions. Studies of these materials have been carried out using conductivity, specific heat measurements, tracer diffusion, x-ray diffusion analysis and infrared reflectivity [1-6].

A_2BX_4 compounds (where A = Tl, Ag, Cu, M = Cd, Hg, Zn, etc.), belong to a class of fast-ionic solids which are promising materials for use in solid state batteries and fuel cells due to extraordinarily high ionic conductivity at supercritical temperatures [7]. Among these substances, the tetrahedrally unit cell of Tl_2HgII_4 is known to be isomorphous with the structure of β-K_2SO_4 at room temperature [8]. Noorussaba at al. [9] from IR measurements on Tl_2HgII_4 has reported these successive vibrational transition between ---cm-1 and ---cm-1.The structural details of the lower phases are not known but I-nuclear quadrupole resonance [8] reveals that the crystal at 77K has higher symmetry than that of the β-K_2SO_4 structure. IR scattering does not provide direct information on the incommensurability but it is well known that near IR there is an activation of extra modes due to change in the optical selection rules [10]. In order to study the dynamics of the mobile ions directly, we have measured the IR spectra of HgI_2 doped $[0.75Tl_2MI_4:0.25AgI]$. Both of these materials are cation conductors with the Hg ions situated in iodine tetrahedral [11].

Thallium batteries or microbatteries can be attractive as power sources for some classes of portable electronic devices operating near room temperature, which may serve as electrolytes in such batteries. Thallium ion conducting composites are interesting materials specially to develop solid-state electrochemical devices such as batteries, fuel cells, sensors, super capacitors, electrochromic display devices, etc. Therefore, in the present study, the investigations are focused on the following alternative novel composite thallium fast ion conductors. In the $[(1-x)\{0.75Tl_2\ MI_4:0.25AgI\}:xHgI_2]$ (where M = Hg, x = 0.2, 0.4, 0.6 and 0.8 mol. wt. %) systems, $[Tl_2MI_4]$ are pure materials, In $[(1-x)\{0.75Tl_2MI_4:0.25AgI\}:xHgI_2]$ (where M = Hg, x = 0.2, 0.4, 0.6 and 0.8 mol. wt. %) composite system $[0.75Tl_2MI_4:0.25AgI]$ considered as host doped with $[xHgI_2]$ (where x = 0.2, 0.4, 0.6 and 0.8 mol. wt. %) as the dopant. The composition of the host was kept constant in all the composite samples of $[(1-x)\{0.75Tl_2MI_4:0.25AgI\}:xHgI_2]$ (where M = Hg, x = 0.2, 0.4, 0.6 and 0.8 mol. wt. %) mixed

composite solid. It has been observed that a much better solid electrolyte composite system can be prepared with the host [$0.75Tl_2MI_4$:0.25AgI] [12].

2. Experimental

2.1. Materials

The following materials were used as received; AgI, TlI and CdI_2 obtained from CDH, HIMEDIA and LOBA CHEMIE (India), with stated purity 99%, 99.99% of 99% respectively.

2.2. Preparation of [(1-x){$0.75Tl_2HgI_4$:0.25AgI}:xHgI_2] composite fast ion conductor

2.2.1. Preparation of pure sample [Tl_2HgI_4].

Thallium tetra mercuro iodate [Tl_2HgI_4] was prepared from TlI and HgI_2 obtained from HIMEDIA and CDH (India), with stated purity 99.99% of 99% respectively by the solid state reactions method. TlI and HgI_2 were mixed in the requisite composition (according to eqn no.1)

$$2TlI + HgI_2 \rightarrow Tl_2HgI_4 \qquad (1)$$

in an Agate mortar and were heated at 116.5°C (388K) for 2.5 days (63 hrs) in an air oven (CE 0434 NSW-144), in silica crucible with intermittent grinding. The rate of heating was initially kept at 50°C per hours for 12 hours. the light orange color compound changed to dark orange color. Tl_2HgI_4 is dark orange color above 110°C -115°C. The color transition from orange to red occurred at 116.5°C and decomposes above 130°C. The resulting material at room temperature was used for further studies [13].

2.2.2. Preparation of host sample [$0.75Tl_2HgI_4$:0.25AgI]

Ag^+-ion doped composite host fast ion conductors were prepared by adding 0.25 mol. wt. % AgI (from CDH 98%) to the pure Tl_2HgI_4 compound. [$0.75Tl_2HgI_4$:0.25AgI] solid solutions was prepared by mixing 0.25 mol. wt. % AgI in pure 0.75 mol. wt. % Tl_2HgI_4, in an Agate mortar at room temperature with intermittent grinding The powder mixture, were ground thoroughly in an Agate mortar and collected in a silica crucible which is then kept in an air oven (CE 0434 NSW- 144) for 24 hours at 100ºC. The resulting material at room temperature was used for further studies [14, 15].

2.2.2. Preparation of doped host sample [(1-x){$0.75Tl_2HgI_4$:0.25AgI}:xHgI_2]

HgI_2 were mixing in various x mol. wt. % (where x = 0.2, 0.4, 0.6, 0.8 mol. wt.%) to the mixture of [$0.75Tl_2HgI_4$:0.25AgI] in (1-x) ratio to form (1-x)[$0.75Tl_2HgI_4$: 0.25AgI]:xHgI_2 by solid state reaction in an Agate mortar and were heated at 100°C (373K) for 2 days (48 hrs) in silica crucible with intermittent grinding. The rate of heating was initially kept at 10°C per hours for 24 hours. After cooling, the dark orrange color compound changed to medium-light orange color in vatious x (where x = 0.2, 0.4, 0.6 and 0.8) mol. wt. % composites. After intermittent grinding, all the samples were prepared and will be used for further studies [14, 16].

2.3. Characterization of [$0.75Tl_2HgI_4$:0.25AgI] and [(1-x){$0.75Tl_2HgI_4$:0.25AgI}:xHgI_2] composite fast ion conductor by FTIR measurements

2.3.1. FTIR measurements

The FTIR spectrum was recorder for the fast ionic composite [$0.75Tl_2HgI_4$:0.25AgI] and [(1-x){$0.75Tl_2HgI_4$:0.25AgI}:xHgI_2] composite system in the mid-infrared range 400-4000 cm^{-1} (25-25 μm) at room temperature using a INTERSPEC-2020, FTIR spectrophotometer measured in KBr. Mid–infrared spectra used to study the fundamental vibrations and associated rotational-vibrational structures.

3. Results and discussion

3.1. FTIR analysis

3.1.1. FAR-IR discussion in [$0.75Tl_2HgI_4$:0.25AgI]

The IR spectrum of the vapour over solid [$0.75Tl_2HgI_4$:0.25AgI] was studied in the 30-700 cm^{-1} region at room temperature are shown in figure 1.

The IR spectrum of [$0.75Tl_2HgI_4$:0.25AgI] solid at room temperature showed two distinct absorption bands. The absorption around 101.43 cm^{-1} shows typical PR band structure of a diatomic molecule and is assigned to the fundamental Tl-I stretching frequency of the monomer. For the band origin at 71.07 cm^{-1} can be attributed to the $(TlI)_2$ dimeric molecule [17]. IR-measurements shows that a sifnificant amount of dimeric molecules is present in the vapour over TlI (I) at the temperature of the present experiments.

Ionic model calculations based on Rittners electrostatic model [18] predicted a square planar structure (D_{2h} symmetry) as the most stable arrangement for $(TlI)_2$. This structure allows three of the total six normal

modes of vibration to be IR active. The B_{2u} and B_{3v} stretching modes involve high frequency in plane motion and the B_{1u} bending mode lower frequency out of plane motion. On the basis of these consideration the peak at 71.07 cm^{-1} is due to the stretching motion and the peak at ca 43.69 cm^{-1} to the bending motion of the $(TlI)_2$ molecule. There is however, no clear argument for the assignment of the observed stretching band to the B_{2u} and B_{3v} mode [18].

The spectrum of [$0.75Tl_2HgI_4$:0.25AgI] solid consisted of two strong absorption bands are listed in Table 1. It is concluded that both peaks are due to HgI_2 molecular species. The linear structure of the HgI_2 molecule ($D_{\infty h}$ symmetry), as established by electron diffraction measurements [19-21], allow two of the total of three fundamental frequencies to be infrared active and consequently, the assignment is straight forward, the symmetric Hg-I stretching frequency υ_3 at 231.80 cm^{-1} and I-Hg-I blending frequency υ_2 at 135.36 cm^{-1}. The additional sharp lines in the spectrum are due to the rotational spectrum of H_2O impurities. The IR spectrum of [Tl_2HgI_4] solid composite, also shows three distinct absorption bands at 324.66, 431.82 and 602.07 cm^{-1}. On further increasing the wavenumber the position of the absorption bands are in excellent agreement with those of the [Tl_2HgI_4] molecules [22] above 400 cm^{-1}, the intensity of the peaks decreases, owing to condensation of HgI_2 in the colder parts of the optical cell, these bands corresponds to those TlI and indicate the presence of TlI and $(HgI_2)_2$ molecules.

In addition, numerous sharp absorption bands of the rotational spectrum of [$0.75Tl_2HgI_4$:0.25AgI] were presents, which were at 160.36, 186.85 and 256.80 cm^{-1}. These absorption bands are in excellent agreement with those of the [$0.75Tl_2HgI_4$:0.25AgI]. Additional peaks that might indicate the presence of AgI species is at 36.25 cm^{-1} have been observed shows Ag-I stretch of the molecule.

The present results shows that the successive release of HgI_2 and $TlI/(HgI_2)_2$ vapour species occurs during heating, pointing towards dissociation of [$0.75Tl_2HgI_4$:0.25AgI] molecules under the conditions of the experiments.

3.1.2. FTIR discussion in [$0.75Tl_2HgI_4$:0.25AgI]

Assuming the β phase is tetragonal, the number and symmetry of normal modes can be determined. Group theory analysis finds the following number and symmetries for the 10 optical modes in Tl_2CdI_4 materials.

Tl_2HgI_4: 3A+ 5B+ 5E

The Infrared and Raman selection rules give the following allowed mode symmetries.

	Infrared	Raman
Tl_2HgI_4:	5B+ 5E (10 Bands)	3A+ 5B+ 5E (13 Bands)

Using projection operators, we find that the B symmetry mode involve motion of the cation along the tetragonal c axis (z), and the E modes involve motion of the cations, along the a and b axes (x or y), B mode couple to electric fields along the z axis and E modes couple to fields in the xy plane, so that FTIR spectra would determine the mode-symmetry assignments uniquely [23-26].

3.1.3. Factor group analysis of [$0.75Tl_2HgI_4$:0.25AgI]

The irreducible representation for the 10 IR allowed modes are listed in Table 1.

The unit cell group analysis of [$0.75Tl_2HgI_4$:0.25AgI] is also shown in Table 2 [25], with the D_{2d} - S_4 correlation being A_1 and A_2 to A, B and B_2 to B and E to E. Figure 2 shows FTIR spectrum for [$0.75Tl_2HgI_4$:0.25AgI] fast ionic conductors. In the IR spectra of [$0.75Tl_2HgI_4$:0.25AgI] the 2924.00 cm^{-1} peak in Table 2 is strongest in xx, yy and zz direction making it an A. The peak at 1628.02 cm^{-1} and 1328.52 cm^{-1} are strongest in the xx and yy polarizations and therefore belongs to A or B classes. The only noticeable peaks in xz polarization and E symmetry is at 490.51 cm^{-1} and the 1062.62 cm^{-1} shoulder appears to be weak in xx, zz and xz polarization making it likely that at least some of the peaks causing this feature would be maximized in the xy polarization and therefore of B symmetry in [$0.75Tl_2HgI_4$:0.25AgI.

Unassigned and a speculatively assignment for the 1062.62 cm^{-1} feature. HgI_2 contamination peaks also found in at 1102.02, cm^{-1} for [$0.75Tl_2HgI_4$:0.25AgI. Peaks of B and E symmetry are allowed in the IR spectra and should be strong peaks. The occurrence of 490.51 cm^{-1} for [$0.75Tl_2HgI_4$:0.25AgI in the IR strengthens the E assignment for the peak at 490.51 cm^{-1}. (Table 1).

3.1.4. FTIR Comparison in [$0.75Tl_2HgI_4$:0.25AgI]

From Table 2, the vibrational modes can be assigned by considering [$0.75Tl_2HgI_4$:0.25AgI] as consisting of the vibrational modes of TlI and $(HgI_4)^{2-}$ species. In fact, as shown in Figure. 2, almost all the bands due to TlI and $(HgI_4)^{2-}$ are seen in the pure Tl_2HgI_4 composites. The band at 1628.02cm^{-1} can be assigned to the symmetric stretching "A" mode of $(HgI_4)^{2-}$ species and this band is the strongest band at room temperature [23]. This assignment is in good agreement with the other $(HgI_4)^{2-}$ tetrahedral compounds [27]. The 1000-1500 cm^{-1} region

consists of bands at the positions 1382.52 cm^{-1} and 1062.62 cm^{-1} at room temperature and at low temperature, these bands are expected to split.

It is known from the IR spectra of [$0.75Tl_2HgI_4$:0.25AgI]-ions conductors that this region consists of mostly of Tl-I [28] stretching modes. Hence, in all [$0.75Tl_2HgI_4$:0.25AgI composite samples, also the bands in this region can be assigned to symmetric stretching modes of Tl -I. Below 700 cm^{-1}, there are five sharp bands at 490.51 in pure [$0.75Tl_2HgI_4$:0.25AgI] [24], it is known from factor group analysis studies [20] that the bands in this region are due to deformation type metal-iodine vibrations. On comparison with $(HgI_4)^{2-}$ species vibrations, the bands at 490.51 cm^{-1} in pure Tl_2HgI_4, can be assigned to Hg-I deformation type bands. The band at 490.51 cm^{-1} in pure [$0.75Tl_2HgI_4$:0.25AgI], is attributed to the E symmetry of Tl^+ translational mode and is the characteristic attempt frequency of Tl^+ ion arising from the diffusive behaviour to oscillatory behaviour. This assignment is well explained by Shriver [26] by referring to the negative pressure dependence and also using theoretical calculations. The value assigned to the attempt frequencies in [$0.75Tl_2HgI_4$:0.25AgI] is similar to cation transition modes [26, 29]. Another possibility is that motion of very large amplitude (diffusive like) is able to create configurational disorder which allows all IR modes [30].

Inspection of Table 2 and Figure. 2, shows that IR spectra of [$0.75Tl_2HgI_4$:0.25AgI] conductors exhibit the strongest feature at ca 1628.02 cm^{-1}, while the infrared activity below 900 cm^{-1} is weak. On the basis of the above discussion, these results strongly suggest that the existence of $(HgI_4)_2^{2-}/(Tl^+)$ tetrahedral in Tl_2HgI_4 ionic conductors should be excluded at least in concentration detectable by infrared spectroscopy [29].

3.2.1. FAR-IR discussion in (1-x)[$0.75Tl_2HgI_4$:0.25AgI]:xHgI_2.

The IR spectrum of the vapour over solid [(1-x){$0.75Tl_2HgI_4$:0.25AgI}:xHgI_2] (where x = 0.2, 0.4, 0.6 and 0.8 mol. wt. %) was studied in the 30-700 cm^{-1} region at room temperature are shown in figure 3.

The IR spectrum of [(1-x){$0.75Tl_2HgI_4$:0.25AgI}:xHgI_2] (where x = 0.2, 0.4, 0.6 and 0.8 mol. wt. %) solid at room temperature showed two distinct absorption bands. The absorption around 105.29 cm^{-1}, 107.59, 109.65, 107.26 cm^{-1} in x = 0.2, 0.4, 0.6 and 0.8 mol. wt. % shows typical PR band structure of a diatomic molecule and is assigned to the fundamental Tl-I stretching frequency of the monomer. For the band origin at 57.27 cm^{-1}, 58.19, 51.18 and 58.59 cm^{-1} in x = 0.2, 0.4, 0.6 and 0.8 mol. wt. % can be attributed to the $(TlI)_2$ dimeric molecule respectively [17]. IR- measurements shows that a sifnificant amount of dimeric molecules is present in the vapour over TlI (I) at the temperature of the present experiments.

Ionic model calculations based on Rittners electrostatic model [18] predicted a square planar structure (D_{2h} symmetry) as the most stable arrangement for $(TlI)_2$. This structure allows three of the total six normal modes of vibration to be IR active. The B_{2u} and B_{3v} stretching modes involve high frequency in plane motion and the B_{1u} bending mode lower frequency out of plane motion. On the basis of these consideration the peak at 57.27 cm^{-1}, 58.19, 51.18, 58.59 cm^{-1} in x = 0.2, 0.4, 0.6 and 0.8 mol. wt. % is due to the stretching motion and the peak at ca 185.69, 183.95, 186.57, 187.13 cm^{-1} in x = 0.2, 0.4, 0.6 and 0.8 mol. wt. % is due to the bending motion of the $(TlI)_2$ molecule. There is however, no clear argument for the assignment of the observed stretching band to the B_{2u} and B_{3v} mode [18].

The spectrum of [(1-x){$0.75Tl_2HgI_4$:0.25AgI}:xHgI_2] (where x = 0.2, 0.4, 0.6 and 0.8 mol. wt. %) solid consisted of two strong absorption bands are listed in Table 4. It is concluded that both peaks are due to HgI_2 molecular species. The linear structure of the HgI_2 molecule ($D_{\infty h}$ symmetry), as established by electron diffraction measurements [19-21], allow two of the total of three fundamental frequencies to be infrared active and consequently, the assignment is straight forward, the symmetric Hg-I stretching frequency υ_3 at 230.94, 230.63, 232.18, 233.12 cm^{-1} in x = 0.2, 0.4, 0.6 and 0.8 mol. wt. % and I-Hg-I blending frequency υ_2 at 143.51 cm^{-1} in x = 0.4, mol. wt. %. The additional sharp lines in the spectrum are due to the rotational spectrum of H_2O impurities. The IR spectrum of [(1-x){$0.75Tl_2HgI_4$:0.25AgI}:xHgI_2] (where x = 0.2, 0.4, 0.6 and 0.8 mol. wt. %) solid composite, also shows three distinct absorption bands at 322.04, 466.65 and 612.46 $cm^{-1,}$ in x = 0.2, 319.72, 467.26 and 617.28 $cm^{-1,}$ in x = 0.4, 321.15, 469.56 and 617.70 $cm^{-1,}$ in x = 0.6 and 321.09, 478.08 and 590.45 $cm^{-1,}$ in x = 0.8. On further increasing the wavenumber the position of the absorption bands are in excellent agreement with those of the [Tl_2HgI_4] molecules [22] above 400 cm^{-1}, the intensity of the peaks decreases, owing to condensation of HgI_2 in the colder parts of the optical cell, these bands corresponds to those TlI and indicate the presence of TlI and $(HgI_2)_2$ molecules.

In addition, numerous sharp absorption bands of the rotational spectrum of [(1-x){$0.75Tl_2HgI_4$:0.25AgI}:xHgI_2] (where x = 0.2, 0.4, 0.6 and 0.8 mol. wt. %) were presents, which were at 264.03 $cm^{-1,}$ in x = 0.2, 183.95, 264.03 in x = 0.4, 161.12, 186.57 and 265.69 $cm^{-1,}$ in x = 0.6 and 187.13, 266.8 $cm^{-1,}$ in x = 0.8.. These absorption bands are in excellent agreement with those of the [(1-x){$0.75Tl_2HgI_4$:0.25AgI}:xHgI_2] (where x = 0.2, 0.4, 0.6 and 0.8 mol. wt. %). Additional peaks that might

indicate the presence of AgI species is at 364.17.45 and 478.08 in x = 0.8 have been observed shows Ag-I stretch of the molecule.

The present results shows that the successive release of HgI_2 and $TlI/(HgI_2)_2$ vapour species occurs during heating, pointing towards dissociation of [(1-x){0.75Tl_2HgI_4:0.25AgI}:xHgI_2] (where x = 0.2, 0.4, 0.6 and 0.8 mol. wt. %) molecules under the conditions of the experiments.

3.2.2. FTIR discussion and Factor group analysis in [(1-x){0.75Tl_2HgI_4:0.25AgI}:xHgI_2]

The unit cell group analysis of [(1-x){0.75Tl_2HgI_4:0.25AgI}:xHgI_2] (where x = 0.2, 0.4, 0.6 and 0.8 mol. wt. %) shown in Figure 4 belongs to the D_{2d} point group. The irreducible representation for the 10 IR allowed modes are listed in Table 5 [25], with the D_{2d} - S_4 correlation being A_1 and A_2 to A, B_1 and B_2 to B and E to E. Figure 4 shows FTIR spectrum for [(1-x){0.75Tl_2HgI_4:0.25AgI}:xHgI_2] (where x = 0.2, 0.4, 0.6 and 0.8 mol. wt. %) fast ionic conductors where x = 0.2,0.4, 0.6 and 0.8 mol. wt. %. In the IR spectra of [0.8{0.75Tl_2HgI_4:0.25AgI}:0.2HgI_2] (where x = 0.2, 0.4, 0.6 and 0.8 mol. wt. %) the 2924.43 cm^{-1} peak in Table 5 is strongest in xx, yy and zz direction making it an A. The A peak shifted in x = 0.4, 0.6 and 0.8 at 2925.71, 2924.79, 2926.36 cm^{-1}. The peak at 1622.53 cm^{-1} and 1385.60 cm^{-1} are strongest in the xx and yy polarizations and therefore belongs to A or B classes. This peak shifted in x = 0.4, 0.6 and 0.8 mol. wt. % composites are 1624.15 and 1382.66 cm^{-1} for x = 0.4, 1621.58 cm^{-1} and 1383.93 for x = 0.6 and 1621.20 and 1388.24 cm^{-1} for x = 0.8 mol. wt. %. The only noticeable peaks in xz polarization and E symmetry is at 420.16 cm^{-1} in x = 0.2 only and the 1053.4 cm^{-1} shoulder appears to be weak in xx, zz and xz polarization making it likely that at least some of the peaks causing this feature would be maximized in the xy polarization and therefore of B symmetry in x = 0.2 mol. wt. %. E symmetry peaks are absent in x = 0.4, 0.6 and 0.8 are at 531.32, 442 and 541.77 cm^{-1}. The shoulder peaks appears in x = 0.2, 0.4, 0.6 and 0.8 are at 1057.63, 1041.34 and 1053.40 respectively. This leaves two weak peaks at 533.27 and 720.67 cm^{-1} in x = 0.2, which shifted in x = 0.4, 0.6, 0.8 mol. wt. % are at 569.75 and 619.18 cm^{-1} in x = 0.4, 518 and 674 cm^{-1} in x = 0.6, 674.28 and 752.94 cm^{-1} in x = 0.8 respectively.
Unassigned and a speculatively assignment for the 531.32 cm^{-1} feature. The band seen at 533.27, 569.75, 518, 674.28 cm^{-1} arises from HgI_2 contamination in x =0.2, 0.4, 0.6, 0.8 mol. wt. % respectively. Also the 720.67, 619.18, 674 and 752.94 cm^{-1} in x = 0.2, 0.4, 0.6, 0.8 mol. wt. % respectively peak may be spurious because it is not observed at low temperature or in room temperature spectra of polycrystalline samples.

3.2.3. FTIR Comparison in [(1-x){0.75Tl_2HgI_4:0.25AgI}:xHgI_2]

The IR active peaks with symmetry assignments are listed in Table 6. For [(1-x){0.75Tl_2HgI_4:0.25AgI}:xHgI_2] (where x = 0.2, 0.4, 0.6 and 0.8 mol. wt. %) in Table 6, 2924.43, 2925.71, 2924.79, 2926.36 cm^{-1} A1 peak is assigned as the HgI_4^{2-} symmetric stretch [25]. Pressure dependence peak at 1622.53, 1624.15, 1621.58 and 1621.20 cm^{-1} resembles that of A symmetry feature in x = 0.2, 0.4, 0.6, 0.8 mol. wt. % respectively [31]. This correlation implies that the 1622.53, peaks in [(1-x){0.75 Tl_2HgI_4:0.25AgI}:xHgI_2] (where x = 0.2, 0.4, 0.6 and 0.8 mol. wt. %) has 1624.15, 1621.58 and 1621.20 cm^{-1} A_1 symmetry in x = 0.2, 0.4, 0.6 and 0.8 mol. wt. % respectively. The peak at 420.16, 531.32, 442, 541.77 cm^{-1} of [(1-x){0.75Tl_2HgI_4:0.25AgI}:xHgI_2] (where x = 0.2, 0.4, 0.6, 0.8 mol. wt. %) can be assigned as B symmetry respectively. Factor group analysis for β-Tl_2HgI_4 shows only two A modes, the HgI_4^{2-} symmetric stretch and a mode which may be described as HgI_4^{2-}symmetric deformation assigned to the (1622.53, 1624.15, 1621.58 and 1621.20) in [(1-x){0.75Tl_2HgI_4:0.25AgI}:xHgI_2] (where x = 0.2, 0.4, 0.6, 0.8 mol. wt. %) composites respectively. This HgI_4^{2-} deformation may be described as a stretch of Hg-I and Ag-I bonds. The broadening of the (1622.53, 1624.15, 1621.58 and 1621.20 cm^{-1} in x = 0.2, 0.4, 0.6, 0.8 mol. wt. %) peaks in β-Tl_2HgI_4, as the temperature is increased toward the temperature of the phase transition also suggests that these modes are associated with Hg-I and Ag-I motion respectively. This behavior contrasts with that of the (2924.43, 2925.71, 2924.79, 2926.36 cm^{-1} in x = 0.2, 0.4, 0.6, 0.8 mol. wt. %) peaks in β-Tl_2HgI_4, respectively, which remain sharp up to the order-disorder phase transitions. The pressure dependence also is consistent with an assignment in which (1622.53, 1624.15, 1621.58 and 1621.20 cm^{-1} in x = 0.2, 0.4, 0.6, 0.8 mol. wt. %) peaks involve thallium iodide motion [13]. In β- Tl_2HgI_4, the Hg-I stretch is contained in a linear modes E (xy_{trans}) – E (xy_{rot}) [32] and possibly one or both of the two weak peaks seen between 3000 and 4000 cm^{-1} at low temperature can be assigned as the Hg-I or Ag-I symmetric stretch (at room temperature). The low frequency modes in β-Tl_2HgI_4 is expected to have several Hg-I and Ag-I deformation with the Hg-I deformations at higher frequency than those of Tl-I. The low frequency E modes at (420.16, 533.27 and 720.67 cm^{-1} in x = 0.2 mol. wt. %, 531.32, 569.75 and 619.18 cm^{-1} in x = 0.4 mol. wt. %, 442, 518 and 674 cm^{-1} in x = 0.6 and 541.27, 674.28 and 752.94 cm^{-1} in x = 0.8 mol. wt. %) in β- Tl_2HgI_4, are of special interest.

Thus this indicates that these modes involve large components of Tl and Ag motions. Accordingly, these E symmetry features are assigned as external Tl^+ or Ag^+ translational modes in the xy plane. The E and B

symmetry coordinates for Tl^+ translation, the former symmetry coordinates corresponds to Tl translation in the xy plane and the latter to Tl translation along the z axis.

A linear combination of the E and B symmetry coordinates may be formed in which cation motion occurs in the direction of the tetrahedral face of four iodide ions. The probable Tl^+ and Ag^+ conduction path involves Tl^+ and Ag^+ motion through this face, into an octahedral site, and through another I_3 triangular face into a tetrahedral site [26]. The values assigned to the attempt frequencies in [(1-x){$0.75Tl_2HgI_4$:0.25AgI}:xHgI_2] (where x = 0.2, 0.4, 0.6 and 0.8 mol. wt. %) are similar to cation translational modes in related electrolytes [26].

Inspection of Table 4 and Figure 4, shows that IR spectra of all [(1-x){$0.75Tl_2HgI_4$:0.25AgI}:xHgI_2] (where x = 0.2, 0.4, 0.6 and 0.8 mol. wt. %), conductors exhibit the strongest feature at ca 1622.53, 1624.15, 1621.58 and 1621.20 cm^{-1} respectively, while the infrared activity below 1000 cm^{-1} is weak. On the basis of the above discussion, these results strongly suggest that the existence of $(HgI_4)_2^{2-}$/(Ag^+:Tl^+) tetrahedral in the x = 0.2, 0.4, 0.6 and 0.8 mol. wt. % (Ag^+:Tl^+)-doped fast ionic conductors should be excluded at least in concentration detectable by infrared spectroscopy.

Therefore, it is found that the infrared activity of the x = 0.2, 0.4, 0.6 and 0.8 mol. wt. % $(HgI_4)_2^{2}$)-fast ionic conductors arises from $(HgI_4)_2^{2-}$ while x = 0.2, 0.4, 0.6 and 0.8 mol. wt. % $(HgI_4)_2^{2}$)-fast ionic conductors show weakest feature at lower frequencies. Increasing the $(HgI_4)_2^{2}$ content induces a decreases to increase of the infrared activity in [(1-x){$0.75Tl_2HgI_4$:0.25AgI}:xHgI_2] (where x = 0.2, 0.4, 0.6 and 0.8 mol. wt. %) [29].

4. Conclusions

Thus, novel composite fast ion conductors [$0.75Tl_2HgI_4$:0.25AgI] and [(1-x){$0.75Tl_2HgI_4$:0.25AgI}:xHgI_2] (where x = 0.2, 0.4, 0.6 and 0.8 mol. wt. %) composite fast ion conductors were prepared and investigated also by FTIR spectral analysis, studies to confirmed the formation of all the fast ion conductors.

Acknowledgements

The authors are gratefully acknowledged to UGC New Delhi for financial assistance as UGC-PDF Women Scientist Scheme. The authors also thankful to Prof. Reshef Tenne and Dr. Feldmann at the Wiezmann Institute of Science (Israel) for obtaining the x-ray measurements of our pure and doped samples. The authors also gratefully acknowledge the Chairman of the Department of Chemistry for providing the research facilities.

Notes and references

[1]. C. Tubandt and Lorenze, Z. Phys. Chem. 87, 513 (1914); owens B. B. And Argue G.R., Science, N.Y. 157, 308 (1967).
[2]. C.M. Perrott and N.H. Fletcher, J. Chem. Phys. 48, 2681 (1967). W. V. Johnston, H. Wiedersich and G.W. Lindberg, J. Chem. Phys. 51, 3739 (1969).
[3]. A. Kvist And R. Z. Tarneberg Naturf 25 a 257 (9170).
[4]. S. Hoshino, J. Phys. Soc. Japan 12, 315 (1957) Gellers, Science, N. Y. 157, 310 (1967).
[5]. K. Funke and A. Jost, Berbunsenges, Phys. Chem., 75 436 (1971).
[6]. G. Eckold and K. Funke, Z. Naturf. 28a, 1042 (1973).
[7]. C.A. Angell, Annu. Rev. Chem. 43 (1992) 693.
[8]. D.E. Scaife, Australian J. Chem. 24, 1315 (1971).
[9]. Noorussaba, Afaq Ahmad Preparation, Crystal Structure, Thermal Properties and Vibrational Modes of Tl2CdI4 Nanocomposite Material, Journal of Nanoscience and technology, 2 (3), (2016), 140-143.
[10]. The Rasing, P. Wyder, A. Janner and T. Janssen, Phys. Rev. B 24, 7504 (1982).
[11]. Wiedersich H. And gellers S., Fast ion transport in solids (edited by Vangool W.), P. 629. North
[12]. R.C. Agrawal, R. Kumar, A. Chandra, Transport studies on a new fast silver ion conducting system: 0.7[0.75AgI:0.25AgCl]:0.3 [yAg_2O:$(1-y)B_2O_3$], Solid State Ionics 84 (1996) 51-60.
[13]. K.I. Avdienko, D.V. Badikov, V.V. Badikov, V.I. Chizhikov, V.L. Panyutin, G.S. Shevyrdyaeva, S.I. Scherbakov, E.S. Scherbakova, Optical Materials, 23 (2003) 569-573.
[14]. Noorussaba, Afaq Ahmad and Reshef Tenne, Central Europian Journal of Chemistry , 8 (6), (2010), 1227-1235.
[15]. Noorussaba, Afaq Ahmad, Ionics, 17, 8, (2011), 759-766.
[16]. A.L. Laskar, S. Chandra, Superionic Solids and Solid Electrolytes: Recent Trends, Academic Press, San Diego, 1989
[17]. V.P. Glushko, L.V. Gurvich, G.A. Bergman, I.V. Veits, V.A. Medvedev, G.A. Khachkuruzov and V.S. Yungman, Termodinamicheskie Svoista Individual nykh Veshchestv, Vol IV, Nauka, Moskow, 1982.
[18]. B.T. Gowda and S.W. Benson, J. Chem. Soc., Faraday Trans. 2, 79, (1983) 663.
[19]. P.A. Akashin and V.P. Spiridonov, Kristallographia, 2 (1957) 472.

[20]. M.W. Listen and L.E. Sutton, Trans. Faraday Soc., 37 (1941) 406.
[21]. O. Hassel and L.C. Stromme, Z. Phys. Chem., 38 (1938) 466.
[22]. R. Viswanathan and K. Hilpert, Ber. Bunsenges. Phys. Chem., 83 (1984) 125.
[23]. M. Hassan, M.S. Nawaz, Rafiuddin, Ionic conduction and effect of immobile cation substitution in binary system (AgI) 4/5–(PbI2) 1/5, Radiat. Eff. Defect. S. 163 (2008) 885-891.
[24]. K. Wakamura, Characteristic properties of dielectric and electronic structures in super ionic conductors, Solid State Ionics 149 (2002) 73–80.
[25]. R. Sudharsanan, T.K.K. Srinivasan, Radhakrishna, Raman and far IR studies on Ag_2CdI_4 and Cu_2CdI_4 superionic compounds, Solid State Ionics 13 (1984) 277- 283.
[26]. A. Viswanathan, S. Austin Suthanthiraraj, Impedance and modulus spectroscopic studies on the fast ion conducting system CuI-Ag_2MoO_4, Solid State Ionics 62 (1993) 79-83.
[27]. J.B. Goodenough, Ceramic solid electrolytes, Solid State Ionics 94 (1997) 17-25.
[28]. S. Geller (ed), Solid Electrolytes (Berlin Springer) 1977.
[29]. E. A. Secco, A. Sharma, Structure stabilization: locking-in fast cation conductivity phase in TlI, J. Phys. Chem. Sol. 2 (1995) 251–254.
[30]. K. Funke, AgI-type solid electrolytes. Progress in Solid State Chemistry, 11 (1976) 345-402.
[31]. H.G. Le Duc and L.B. Coleman, Far-infrared studies of the phase transition and conduction mechanism in the fast-ion conductors Ag_2HgI_4 and Cu_2HgI_4, Physical Review B, 31 (1985) 933-941.
[32]. P. Knauth, Ionic Conductor Composites: Theory and Materials, Journal of Electroceramics, 5 (2000) 111-125.

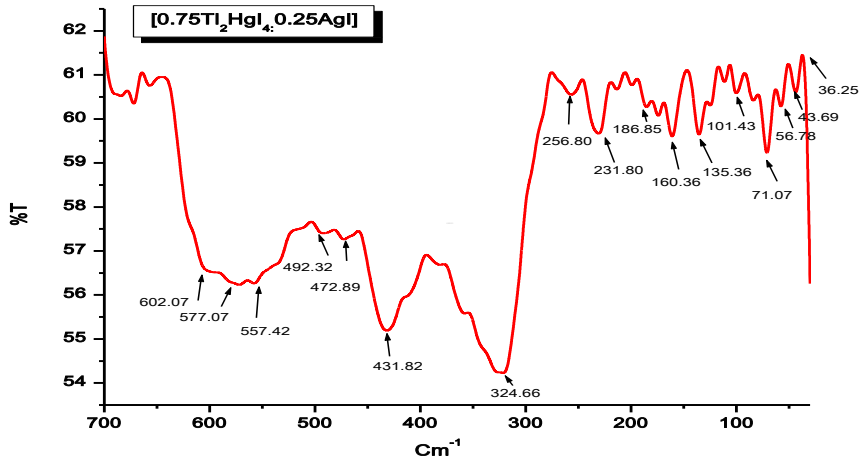

Fig. 1. FAR-IR spectrum for [0.75Tl_2HgI_4:0.25AgI] fast ionic conductors.

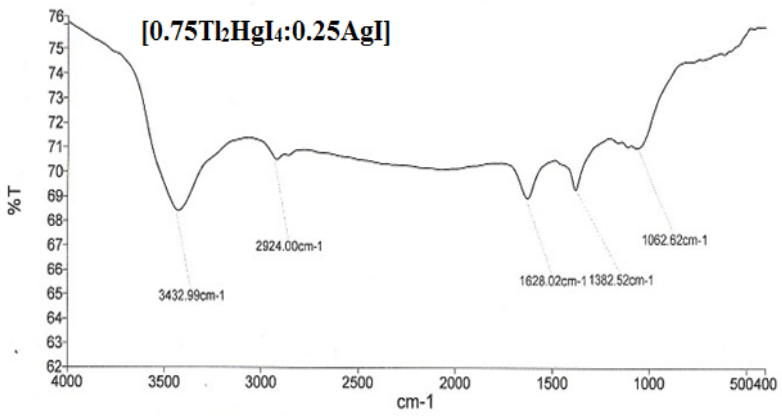

Fig. 2. FTIR spectrum for. [0.75 Tl_2HgI_4:0.25AgI])] fast ionic conductors.

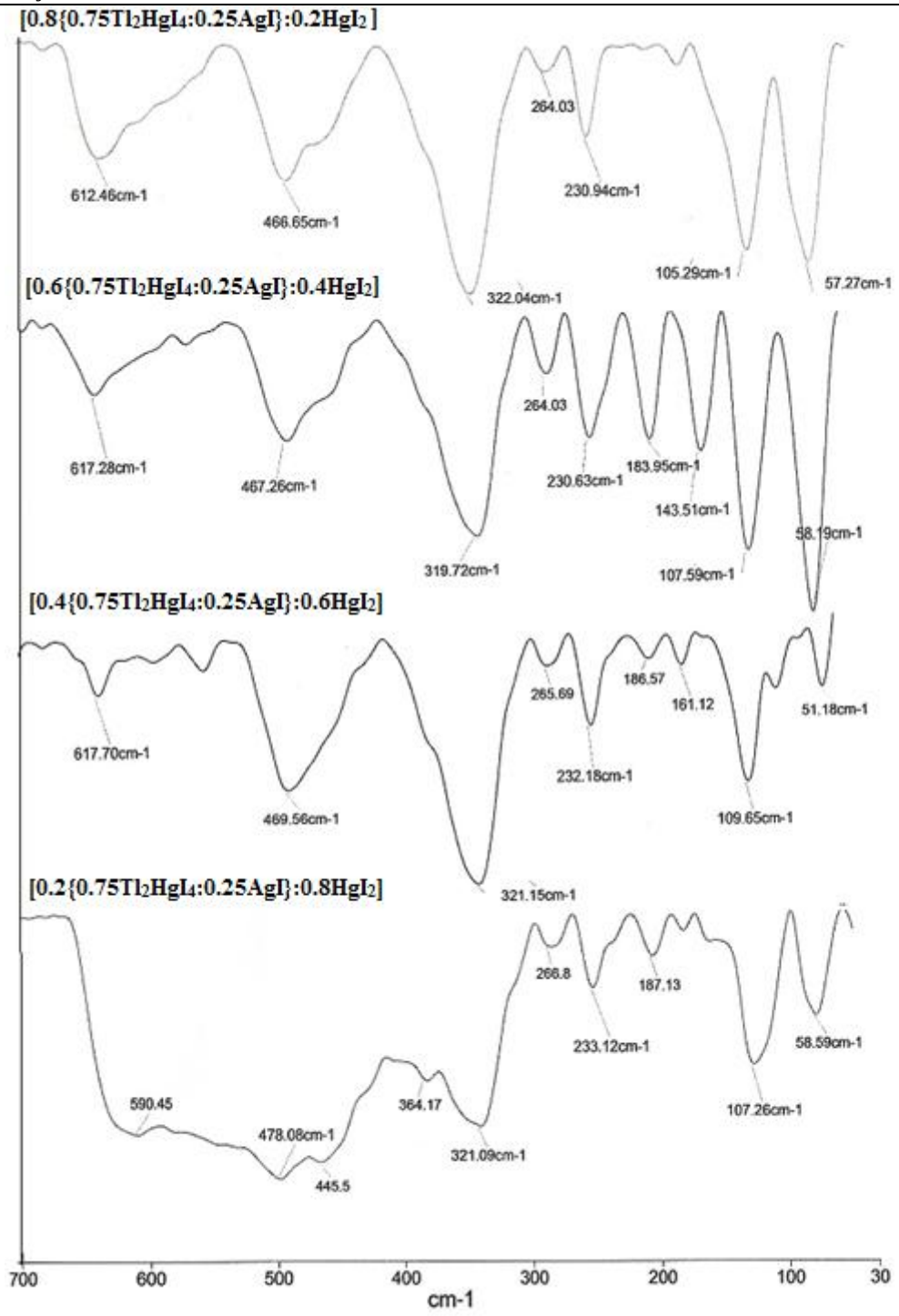

Fig. 3. FAR-IR spectrum for $[(1-x)\{0.75Tl_2HgI_4:0.25AgI\}:xHgI_2]$ (where x = 0.2, 0.4, 0.6 and 0.8 mol. wt. %) fast ionic conductors.

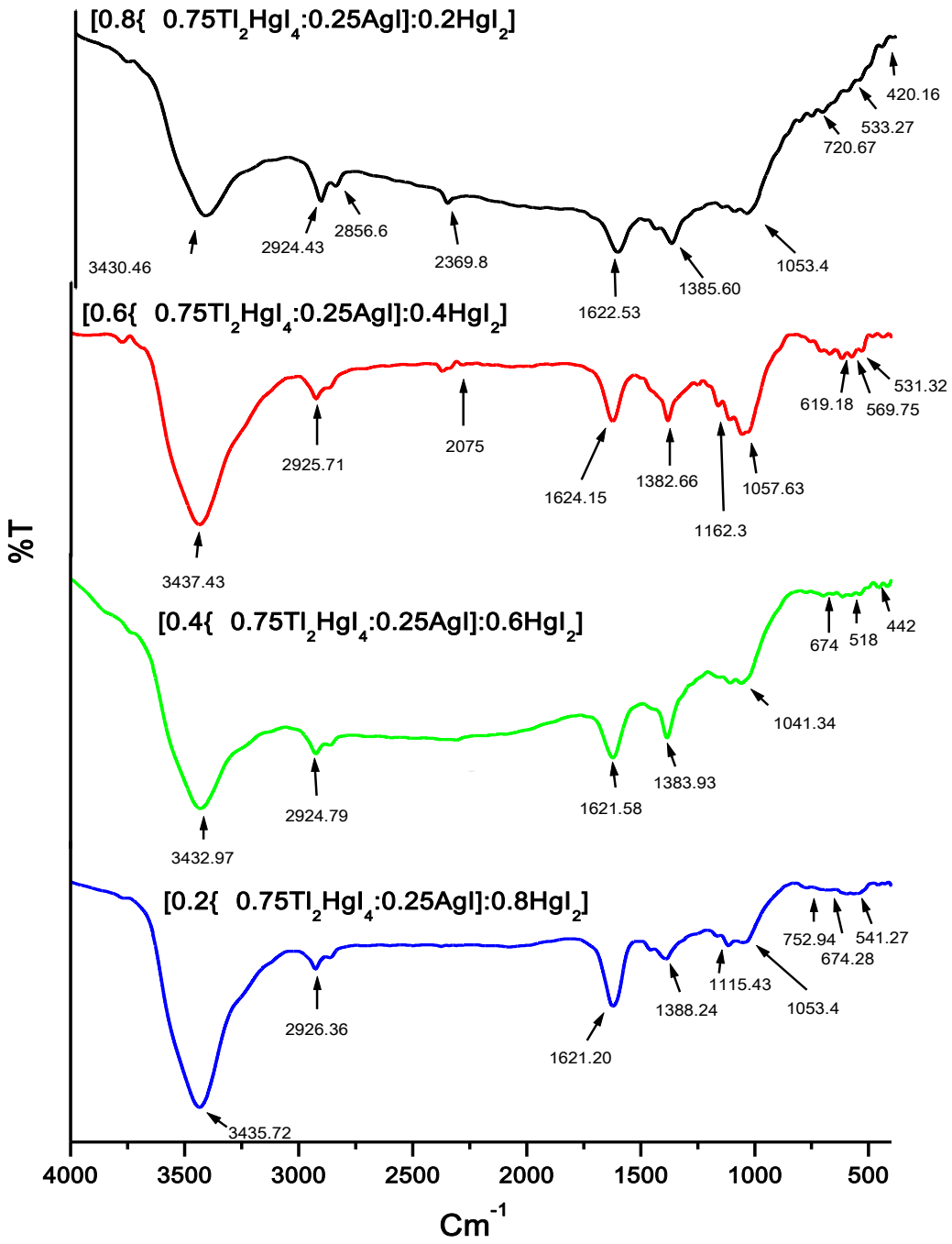

Fig. 4. FTIR spectrum for $[(1-x)\{0.75Tl_2HgI_4:0.25AgI\}:xHgI_2]$ (where x = 0.2, 0.4, 0.6 and 0.8 mol. wt. %) fast ionic conductors.

Table 1. FAR-IR bands in [0.75Tl_2HgI_4:0.25AgI] and assignments

[0.75Tl_2HgI_4:0.25AgI]			
Compound	**Value (cm^{-1})**	**Assignment**	**nature**
TlI	101.43	ω_e	TlI stretch of the monomer
	71.07	B_{2u} and B_{3v}	stretching motion of $(TlI)_2$ dimeric molecule
	43.69	B_{1u}	bending motion of the $(TlI)_2$ molecule
HgI_2	231.80	υ_3	symmetric Hg-I stretch of the dimer
	135.36	υ_2	I- Hg-I blend
Tl_2HgI_4	324.66	___	Dissociation of Tl_2HgI_4 molecule
	431.82	___	TlI - stretch
	602.07	___	$(HgI_2)_2$ -stretch
AgI Tl_2HgI_4-AgI	36.25 160.36 186.85 256.80	----- ___ ___ ___	Ag-I stretch of the molecule formation of the [0.75Tl_2HgI_4:0.25AgI] band formation of the [0.75Tl_2HgI_4:0.25AgI] band formation of the [0.75Tl_2HgI_4:0.25AgI] band

Table 2. [0.75Tl_2HgI_4:0.25AgI] fast ionic conductors room temperature peaks and assignments.

[0.75Tl_2HgI_4:0.25AgI] (cm^{-1})	**Symmetry**	**Assignments**
2924.00	A	$(HgI_4)^{-2}$ symmetric stretch respectively
1100.02		Tl-I and Hg-I symmetric stretch
1628.02	A	$(HgI_4)^{-2}$ deformation, M-I stretching
1062.62	?	Deformation
1382.52	B	
490.51	E	weak in xx, zz and xz polarization

frequency

Table 3. **[0.75Tl_2HgI_4:0.25AgI] fast ion conductors, room temperature peaks and assignment.**

FTIR transmission peaks (cm^{-1})		
[0.75Tl_2HgI_4:0.25AgI] (cm^{-1})	**Symmetry**	**Assignment**
2924.00	A	HgI_4^{2-} Symmetric stretch
1628.02	A	HgI_4^{2-} deformation, M-I stretching
1062.62	?	deformation
1382.52	B	Tl-I , Ag-I symmetric stretch
490.51	B	Tl^+attempt frequency

Table 4. FAR-IR bands in [(1-x){0.75Tl_2HgI_4:0.25AgI}:xHgI_2] and assignments

Compound	**[0.8{0.75Tl_2HgI_4: 0.25AgI}:0.2HgI_2]**	**[0.6{0.75Tl_2HgI_4: 0.25AgI}:0.4HgI_2]**	**[0.4{0.75Tl_2HgI_4: 0.25AgI}:0.6HgI_2]**	**[0.2{0.75Tl_2HgI_4: 0.25AgI}:0.8HgI_2]**	**Assignments**	**nature**
Tl-I	105.29 57.27	109.81 73.35	109.81 73.35	109.81 73.35	ω_e υ_5	Tl-I stretch of the monomer Assymmetric Cd-I stretch of the dimer
HgI_2		230.63 143.51	232.18 141.20	233.12 144.40	υ_3 υ_z	Assymmetric Cd-I stretch of the dimer I-Cd-I blend
Tl_2HgI_4	322.04 466.65 612.46	319.72 467.26 617.28	321.15 469.56 617.70	321.09 478.08 590.45	- - -	Dissociation of the [Tl_2CdI_4] molecule Tl-I stretch $(CdI_2)_2$ stretch
AgI Tl_2HgI_4-AgI	160.99 182.38 264.03	143.51 183.95 264.03	161.12 186.57 265.69	159.08 187.13 266.8	- - -	Ag-I stretch of the molecule formation of the [(1-x){0.75Tl_2HgI_4:0.25AgI}:xHgI$_2$] band formation of the [(1-x){0.75Tl_2HgI_4:0.25AgI}:xHgI$_2$] and

Table 5. **[(1-x){0.75Tl_2HgI_4:0.25AgI}:xHgI_2] (where x = 0.2, 0.4, 0.6 and 0.8 mol. wt. %.) room temperature peaks and assignments.**

[0.8{0.75Tl_2HgI_4:0.25AgI}:0.2HgI_2]		**[0.6{0.75Tl_2HgI_4:0.25AgI}:0.4HgI_2]**		**[0.4{0.75Tl_2HgI_4:0.25AgI}:0.6HgI_2]**		**[0.2{0.75Tl_2HgI_4:0.25AgI}:0.8HgI_2]**	
Peaks (cm^{-1})	Assignments	Peaks (cm^{-1})	Assignments	Peaks (cm^{-1})	Assignments	Peaks (cm^{-1})	Assignments
2924.43	A	2925.71	A	2924.79	A	2926.36	A
1622.53	A	1624.15	A	1621.58	A	1621.20	A
1053.4	?	1057.63	?	1041.34	?	1053.40	?
1385.60	B	1382.66	B	1383.93	B	1388.24	B
420.16	B	531.32	B	442	B	541.77	B

Table 6. [(1-x){0.75Tl_2HgI_4:0.25AgI}:xHgI_2] fast ion conductors, where (x = 0.2, 0.4, 0.6 and 0.8 mol. wt. %), room temperature peaks and assignment.

FTIR transmission peaks (cm^{-1})					Assignment
[0.8{0.75Tl_2HgI_4:0.25AgI:0.2 HgI_2]	**[0.6{0.75 Tl_2HgI_4: 0.25AgI} :0.4HgI_2]**	**[0.4{0.75 Tl_2HgI_4: 0.25AgI} :0.6HgI_2]**	**[0.2{0.75 Tl_2HgI_4: 0.25AgI} :0.8HgI_2]**	**Symmetry**	
2924.43	2925.71	2924.79	2926.36	A	HgI_4^{2-} Symmetric stretch
1622.53	1624.15	1621.58	1621.20	A	HgI_4^{2-} deformation, M-I stretching
1053.4	1057.63	1041.34	1053.40	B	deformation
1385.60	1382.66	1383.93	1388.24	E	Tl-I , Ag-I symmetric stretch
420.16	531.32	442	541.77	E	Tl^+ , Ag^+ attempt frequency